Monthly Monitoring of Land Cover Change from Barren Land to Built-up Areas Using RADARSAT-2 PolSAR Images

Zhixin Qi and Anthony G.O. Yeh

The University of Hong Kong
email corresponding author: qizhixin@connect.hku.hk

Abstract

There are many illegal land developments at the urban fringe in developing countries that are experiencing a process of rapid urbanization. Monthly monitoring of land cover change from barren land to built-up areas is important for local governments to detect and prevent illegal land developments at the early stage. Polarimetric synthetic aperture radar (PolSAR), which is not affected by clouds and outperform single-polarization SAR in land cover classification, is therefore a promising tool for the monitoring of monthly land cover changes. However, seasonal growth of agricultural and natural vegetation may obscure changes from barren land to built-up areas because some vegetation are easily confused with buildings in PolSAR images due to the similar scattering mechanism. The objective of this study is to explore a new method for discriminating monthly changes to built-up areas from changes caused by seasonal vegetation growth. Three sequential repeat-pass RADARSAT-2 PolSAR images with a repeat cycle of 24 days were used in this study. Change detection between the first and second images was made to detect monthly land cover changes, and then the interferometric coherence between the second and third images was extracted to improve the change detection result of the first and second images by reducing the confusion between changes to built-up areas and changes caused by seasonal vegetation growth. Within the time interval between the second and third images, change areas caused by seasonal

vegetation growth significantly lost coherence as a result of vegetation growth, while the coherence of built-up areas remains high. Improved with the interferometric coherence, the detection accuracy for changes from barren land to built-up areas increased from 78.61% to 85.03%, while the false alarm rate reduced from 0.25% to 0%. The results showed that interferometric coherence is effective in distinguishing monthly changes from barren land to built-up areas and changes caused by seasonal vegetation growth.

1. Introduction

There are many illegal land developments at the urban fringe in developing countries that are experiencing a process of rapid urbanization. Some illegal land developments have caused irreversible environmental problems such as forest degradation, soil erosion, and disappearance of species diversity (Yeh and Li, 1996). Most illegal land developments are related to land cover change from barren land to built-up areas. Monthly monitoring of this type of change is important for local governments to detect and prevent illegal land developments at the early stage. Remote sensing data obtained from different optical sensors have been commonly used to characterize and quantify land cover information. However, conventional optical remote sensing is limited by weather conditions, and thus has difficulties in collecting timely land cover information in regions frequently covered by clouds. Radar remote sensing, which is not affected by clouds, is therefore promising for monthly monitoring of land cover changes in those regions.

Early studies on land cover investigation with radar remote sensing were mainly performed using airborne radar imagery, such as SIR-C/X-SAR (Saatchi et al., 1997). Despite the promising results of these studies, regular land cover investigation using airborne radar imagery was impractical because airborne radar imagery systems were only occasionally launched for collecting experimental data. The use of radar remote sensing in regular land cover investigation has become practical since some operational orbital synthetic aperture radar (SAR) systems, such as RADARSAT-1, ERS-1 and ERS-2, and JERS-1, were made available for collecting data regularly. However, most orbital SAR systems are single-frequency types. Though useful, when taken alone, each of these orbital SARs may create confusion during mapping and separation of land cover classes. This confusion can mainly stem from limited spectral information obtained by single-frequency SAR systems (Ulaby et al., 1986). In order to overcome the

difficulty of single-frequency SAR data, some studies used PolSAR images to investigate land cover information (Pierce et al., 1994). The results indicate that PolSAR images produce better classification results than single-polarization SAR images.

Numerous methods for change detection that use remote sensing data have been developed in past studies. Reviews of existing change detection methods can be found in many papers (Lu et al., 2004). Image differencing and post-classification comparison (PCC) are the most widely used change detection approaches. The image differencing is relatively simple, straightforward, and easy to implement and interpret. However, this approach cannot provide information on the types of change. PCC can provide information on both change areas and the types of change these areas undergo. However, the accuracy of PCC is limited by the accuracy of the independent classification. In addition, most change detection methods are performed on the pixel level. When applied to PolSAR images, pixel-based methods have two disadvantages. First, they are prone to be affected by the speckle in PolSAR images and produce errors (Qi et al., 2012). Second, they are difficult to use to extract and utilize spatial and textural information, which is helpful in improving classification accuracy of remote sensing data (Gao et al., 2006).

A new hybrid method that integrates change vector analysis (CVA), PCC, and object-oriented image analysis has been recently developed for land cover change detection using RADARSAT-2 PolSAR images (Qi and Yeh, 2012). CVA was applied to identify change areas, and then PCC was used to determine the type of changes. The hybrid method can reduce the impact of each individual classification on the change detection result and then provide information on types of change. Furthermore, it can reduce the speckle effect and utilize textural and spatial information by performing change detection on the object level. Although this method is effective in detecting land cover changes, seasonal growth of agricultural and natural vegetation may still pose difficulties for monthly monitoring of land cover changes. Some vegetation is easily confused with buildings in PolSAR images because of the similar scattering mechanism, and it may be difficult to discriminate land cover changes to built-up areas from changes caused by seasonal vegetation growth.

The objective of this study is to explore a new method to discriminate monthly changes to built-up areas from changes caused by seasonal vegetation growth using RADARSAT-2 PolSAR images. Three sequential repeat-pass images with a repeat cycle of 24 days were used in this study. Change detection between the first and second images was made to detect monthly land cover changes, and then the interferometric coherence between the second and third images was extracted to improve the change

detection result of the first and second images by reducing the confusion between changes to built-up areas and changes caused by seasonal vegetation growth. Croplands and natural vegetation are significantly influenced by temporal decorrelation and lose coherence within a few days or weeks as a result of growth, movement of scatterers, and changing moisture conditions. In contrast, within built-up areas, coherence remains high even between image pairs separated by a long time interval.

2. Study area and data

The study area is located in Panyu District of Guangzhou City in Southern China. Panyu has a total land area of 1,314 km^2 as well as a population of 926,542. This district was an agricultural area before the economic reform in 1978, but has been transformed recently into a rapidly urbanized area. Since Panyu became a district of Guangzhou in July 2000, intensive land development has been implemented to provide housing to the residents of Guangzhou City. Huge profits have been generated through property development, which resulted in the increase in land speculation activities and illegal land developments.

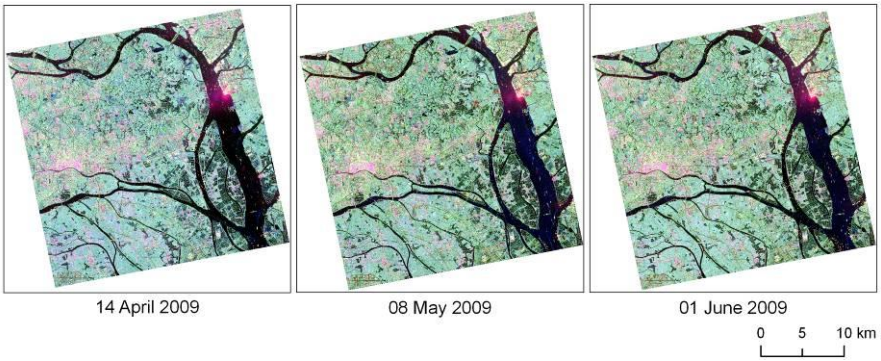

Fig. 1. RADARSAT-2 PolSAR images used for monitoring monthly land cover changes from barren land to built-up areas (Pauli RGB composition)

Three sequential repeat-pass RADARSAT-2 PolSAR images with fine quad-pol (FQ12) and Single Look Complex (SCL) acquired on April 14, 2009, May 08, 2009, and June 01, 2009 were used in this study (Figure 1). The images have a full polarization of HH, HV, VH, and VV, a resolution of 5.2 × 7.6m, and an incidence angle of 31.5 degrees. Land cover classes in the study area can be summarized into five categories: built-up areas (UB), vegetation (V), paddy (P), water (W), and barren land (BL). To

evaluate change detection results, samples of different types of land cover change and no-change areas were selected through visual interpretation and field investigations. Visual interpretation was first conducted to identify change and no-change areas from the entire coverage of images. After that, field investigations were carried out to validate the identified change areas. The number of plots of different types of land cover change was close to that of actual change. Table 1 shows the number of pixels selected for each type of land cover change and no-change.

Table 1. Number of pixels of each type of change and no-change

		Pixels
Change	Barren land -Built-up areas	1,543
	Barren land - Vegetation	1,484
	Barren land - Water	1,331
	Barren land - Paddy	5,365
	Vegetation - Barren land	2,709
	Vegetation - Water	1,434
	Water - Barren land	7,748
	Water - Vegetation	472
	Water - Paddy	3,890
	Paddy- Paddy	3,623
	Total	29,599
No-change (NC)		373,325

3. Methodology

Three sequential repeat-pass RADARSAT-2 PolSAR images were used to detect land cover changes from barren land to built-up areas. Change detection between the first and second images was performed to detect monthly land cover changes, and then the change detection result was improved by reducing the confusion between changes to built-up areas and changes caused by seasonal vegetation growth using the interferometric coherence extracted from the second and third images. Figure 2 shows the methodology of monthly monitoring land cover changes from barren land to built-up areas.

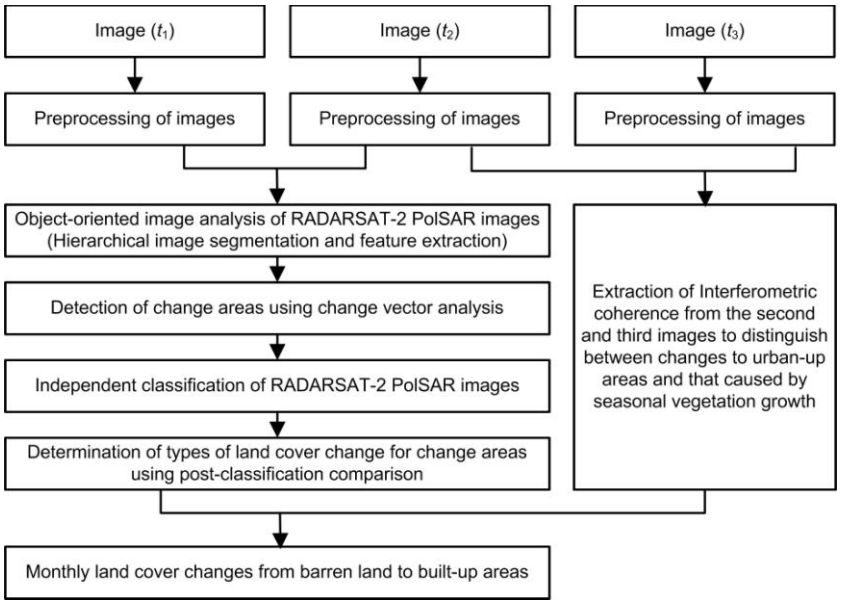

Fig. 2. Methodology of monthly monitoring land cover changes from barren land to built-up areas

3.1. Preprocessing of RADARSAT-2 PolSAR images

Image preprocessing, which is critical to change detection, included radiometric correction, speckle filtering, and image registration. Radiometric calibration for the images was performed using PolSARPro_v4.1.5 software (López-Martínez, 2005) and applying the sigma look-up table provided in the product. After radiometric correction, the pixel values of the images could be directly related to the radar backscatter of the scene. This is necessary for the comparison of PolSAR images acquired from the same sensor but at different times. A J.S. Lee Sigma filter with a window size of 7×7 was applied on the images to reduce speckles. Compared with other filters, this one effectively retains subtle details and preserves the shape of small land parcels while reducing the speckle effect (Lee et al., 2009). The advantage of this filter will benefit the accurate delineation of tiny land parcels in object-oriented image analysis. Image registration was based on the geometric rectification of the RADARSAT-2 images. The PCI Geomatica software was used to implement the geometric rectification of the images. The RADARSAT-2 image package provides a total of 180 tie

points evenly distributed across the entire image. These tie points tie the line/pixel positions in image coordinates to geographical latitude/longitude and can be used as ground control points (GCP) to register an image to a geocoded target image. This work first created a master geocoded image with the same resolution as the RADARSAT-2 images and then registered the RADARSAT-2 images to this geocoded master image using PCI Geomatica based on the tie points. Visual inspection indicates that the RADARSAT-2 images were registered perfectly.

3.2. Detection of monthly land cover changes between the first and second images

The method that integrates CVA, PCC, and object-oriented image analysis (Qi and Yeh, 2012) was used to detect land cover changes from the first and second images. Object-oriented image analysis can be used to reduce the speckle effect and extract textural and spatial information to support PolSAR image classification. In object-oriented image analysis, image objects (groups of pixels) are first delineated by using image segmentation techniques, and then change detection and classification are implemented on the object level. The object-oriented package Definiens Developer 7.0 was used to implement the object-oriented image analysis of RADARSAT-2 images. The multi-resolution segmentation module provided by Definiens Developer 7.0 was used to perform image segmentation based on shape and color homogeneity. For change detection, the hierarchical image segmentation procedure was used to minimize the inconsistency in delineating objects from two successive images (Qi and Yeh, 2012). In considering two co-registered images, image (t_1) and image (t_2), acquired over the same area at different times t_1 and t_2, the procedure of hierarchical segmentation can be summarized as follows: (1) the initial segmentation is applied to image (t_1) with a fixed scale parameter; and (2) the same segmentation process is implemented again on image (t_2) while the segmentation result of image (t_1) is taken as the thematic layer for constraint. This procedure causes all object-merging to take place within the boundaries of the segmentation of image (t_1). As shown in Figure 3, new objects are only created in places where the two images are significantly different (e.g., the red polygon in Figure 3). The hierarchical segmentation technique could eliminate inconsistencies in delineating image objects from two successive images.

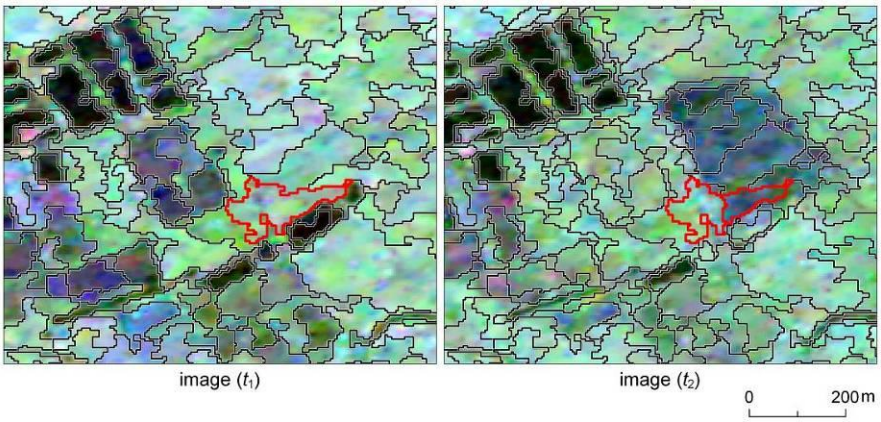

Fig. 3. Hierarchical segmentation for delineating image objects from two successive RADARSAT-2 PolSAR images

After the delineation of image objects, CVA and PCC were used to detect land cover changes on the object level. CVA is a widely used unsupervised change detection method that uses multichannel images (Malila, 1980). CVA can process any number of image channels and can produce detailed change detection information based on the channel change vector obtained by subtracting corresponding image channels of two images acquired at different times. In this study, CVA was used to detect change objects based on selected features instead of pixel values of image channels, and feature change vectors (FCVs) were obtained by subtracting corresponding feature vectors of an image object in two images acquired at different dates. The change magnitude was also computed from FCVs. The higher the change magnitude is, the more likely that changes take place. A widely accepted assumption is that the statistical distribution of the pixels of change and no-change areas in the change magnitude can be approximated as a mixture of Gaussian distributions (Bovolo and Bruzzone, 2007). Therefore, the expectation-maximization (EM) algorithm was applied on the change magnitude to identify change objects. EM is frequently used for data clustering in machine learning and computer vision because it finds clusters by determining a mixture of Gaussians that fit a given data set (Moon, 1996). The Weka 3.6 software (Witten et al., 2011) was used to implement EM algorithms to determine the threshold to identify change objects. Figure 4 shows the change magnitude and the change areas detected from the first and second images.

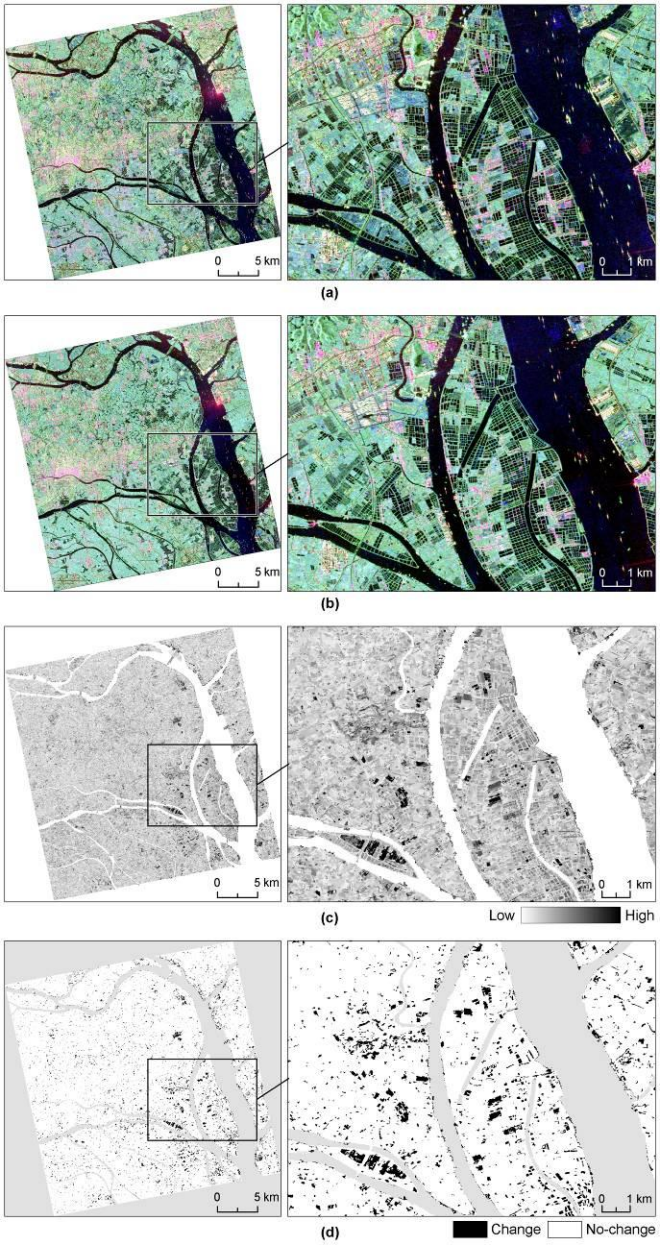

Fig. 4. (a) Image acquired on April 14, 2009, (b) image acquired on May 08, 2009, (c) change magnitude calculated using CVA, (d) change areas detected using EM from the change magnitude

After change areas were detected using CVA, PCC was performed on the change areas to determine the type of changes. Many classification methods for PolSAR data have been explored. However, so far most of the classification methods are pixel-based. These methods are prone to be affected by speckles in PolSAR images and are hard to utilize textural and spatial information. Moreover, they cannot take fully use of polarimetric information of PolSAR data for land cover classification. Qi et al. (2012) proposed a new classification method, which integrates polarimetric decomposition, PolSAR interferometry, object-oriented image analysis, and decision tree algorithms, for the classification of PolSAR images. The results show that the proposed method can achieve much higher accuracy than conventional pixel-based classification methods. This study used this method to implement the classification of RADARSAT-2 PolSAR images. Considering change detection, PolSAR intererometry was not used in the classification. After the independent classification of images, PCC was performed on the change areas to determine the type of changes. Land cover changes detected from the first and second images are shown in Figure 5.

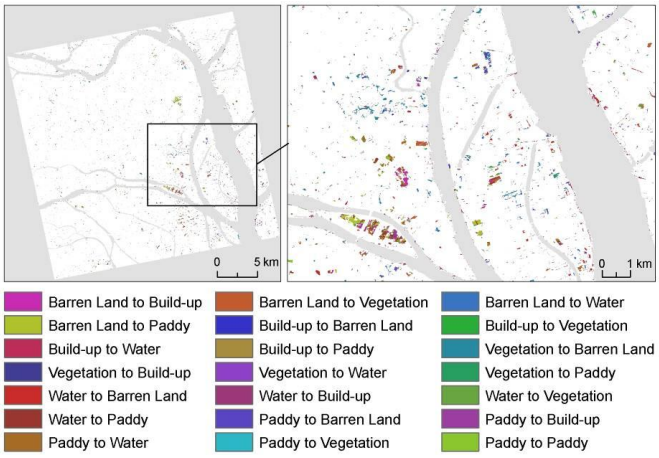

Fig. 5. Land cover changes detected from the first and second images

3.3. Interferometric coherence between the second and third images for improving the change detection result

Seasonal growth of agricultural and natural vegetation may pose difficulties for monitoring land cover changes from barren land to built-up areas. Some agricultural and natural vegetation are easily confused with build-

ings in PolSAR images because of the similar scattering mechanism. Therefore, land cover changes caused by seasonal vegetation growth may obscure changes to built-up areas. Interferometric information has potential to reduce the confusion between changes to built-up areas and changes caused by season vegetation growth. Within the repeat cycle of RADARSAT-2, changes caused by seasonal vegetation growth significantly lost coherency as a result of vegetation growth and changing moisture conditions, while the coherency of changes to built-up areas remains high.

The complex polarimetric interferometric coherence γ as a function of the polarization of the two images has been given by (Papathanassiou and Cloude, 2001). Papathanassiou and Cloude (2001) calculated three optimum complex polarimetric interferometric coherences—γ_{opt_1}, γ_{opt_2}, and γ_{opt_3}—by determining the combination of polarizations that yields the highest coherence. Three polarimetric interferometric parameters (γ_{opt_1}, γ_{opt_2}, and γ_{opt_3}) were extracted from the second and third images (Figure 6). As shown in Figure 6, there is a strong contrast between urban and nonurban areas. The repeat cycle of RADARSAT-2 is 24 days, which produces a very strong temporal decorrelation for nonurban areas, such as croplands and natural vegetation. Croplands and natural vegetation are significantly influenced by temporal decorrelation and lose coherence within a few days or weeks as a result of growth, movement of scatterers, and changing moisture conditions. In contrast, within built-up areas, coherence remains high even between image pairs separated by a long time interval. Qi et al., (2012) indicated that γ_{opt_2} is appropriate for distinguishing between urban areas and nonurban areas. Therefore, this study performed unsupervised classification on γ_{opt_2} to discriminate changes to built-up areas from seasonal vegetation changes.

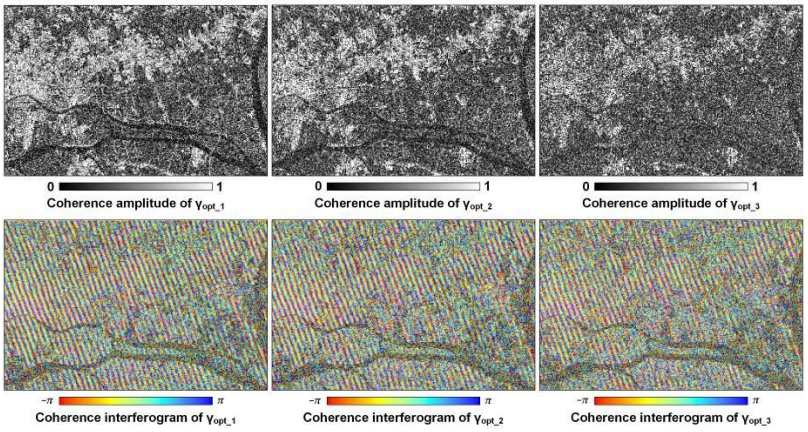

Fig. 6. Optimal complex coherences extracted from the second and third images

4. Results and discussion

The confusion matrix of change type determination in land cover change detection of the first and second images is shown in Table 2. Detection accuracy, false alarm rate, and overall error rate are commonly used statistics for evaluating change detection results. The detection accuracy is the percentage of correctly labeled "change" samples. The false-alarm rate is the percentage of erroneously labeled "no-change" samples. The overall error rate is the percentage of erroneously labeled validation samples. Using the confusion matrix in Table 2, we calculated the detection accuracy, false-alarm rate, and overall error rate for land cover changes from barren land to built-up areas (Table 4). As shown in Table 2, many changes from barren land to paddy or vegetation fields caused by seasonal paddy and vegetation growth were mistakenly identified as change from barren land to built-up areas. Paddies in the study area have two growth cycles a year. The first growth cycle is usually from early April to late July, and the second growth cycle is from early August to early October. Paddy fields usually turn into barren land during the other time periods. During the growth of paddies, the total backscatter from the paddy fields includes the return scattered from the paddy crown, those scattered from the water beneath, and those from the multiple scattering between paddy crown and water surface. Many paddy fields in the study area were barren land on April 14, 2009. With the growth of the paddy, double-bounce scattering from paddy-water surface increased, and paddy fields were easily confused with built-up areas on May 08, 2009 due to the similar scattering mechanism. Therefore, paddy growth caused many false alarms to change from barren land to built-up areas. For the same reason, some other vegetation also produced false alarms to the detection of changes to built-up areas.

Interferometric coherence extracted from the second and third images was used to distinguish barren land to built-up areas from seasonal paddy and vegetation changes. Paddy and vegetation fields are significantly influenced by temporal decorrelation and lose coherence within a few days or weeks as a result of growth, movement of scatterers, and changing moisture conditions. In contrast, within built-up areas, coherence remains high even between image pairs separated by a long time interval. Thus, when considering the urban landscape, baseline decorrelation is the dominant factor, and coherence is reduced to a lesser degree by temporal and other factors which are independent of baseline. As shown in Figure 7, change areas to built-up areas have high coherence amplitude, while changes caused by paddy or vegetation growth have low coherence amplitude. Hence, the coherence image calculated from the second and third im-

ages can be used to improve the change detection result of the first and second images by discriminating changes to built-up areas from changes caused by paddy or vegetation growth. Table 3 shows the confusion matrix of change type determination improved with interferometric coherence. Mistakenly labeled changes caused by seasonal vegetation growth, such as changes from barren land to vegetation or paddies, could be completed eliminated from changes to built-up areas because of their low coherence. Furthermore, some changes to built-up areas that were mistakenly identified as changes to vegetation could be corrected. Consequently, as shown in Table 4, the detection accuracy was increased by 6.42%, while the false alarm rate and overall error rate reduced by 0.25% and 0.28 respectively.

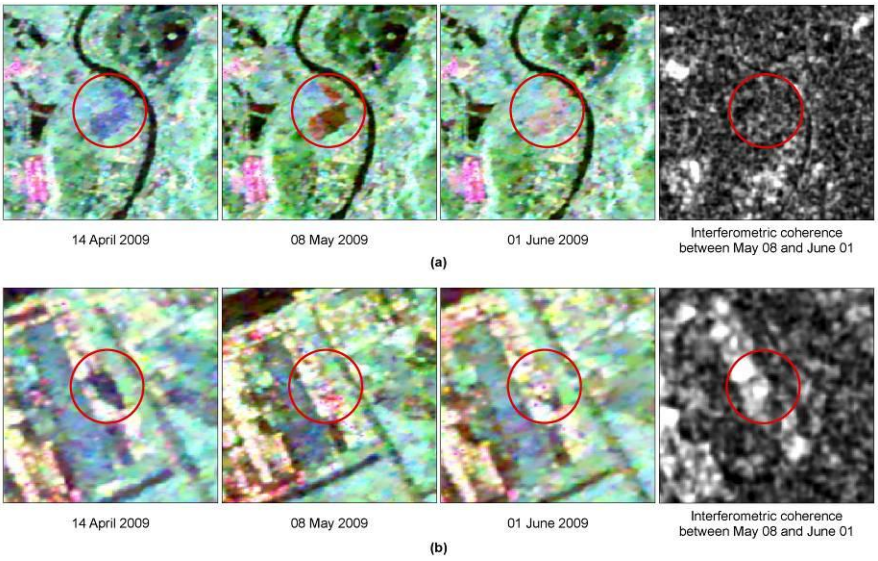

Fig. 7. (a) Change areas caused by paddy growth have low coherence amplitude, (b) change areas from barren land to built-up areas have high coherence amplitude

Table 2. Confusion matrix of change type determination in land cover change detection of the first and second images

Classified data	Reference data																				
	NC	BL-UB	BL-V	BL-W	BL-P	UB-BL	UB-V	UB-P	V-BL	V-UB	V-W	V-P	W-BL	W-UB	W-V	W-P	P-BL	P-UB	P-V	P-P	Total
BL-UB	51	1,213	199	0	0	0	0	0	0	80	0	0	0	0	0	0	0	0	0	0	1,543
BL-V	31	389	1,057	0	0	0	4	0	0	0	0	0	0	0	3	0	0	0	0	0	1,484
BL-W	401	0	0	804	0	0	0	0	111	0	9	0	5	0	0	0	1	0	0	0	1,331
BL-P	61	450	468	0	4,270	0	9	0	0	4	0	48	0	0	16	0	0	0	25	14	5,365
V-BL	298	0	0	0	0	12	0	0	2,399	0	0	0	0	0	0	0	0	0	0	0	2,709
V-W	0	0	0	361	0	0	0	0	0	0	1,073	0	0	0	0	0	0	0	0	0	1,434
W-BL	456	0	56	0	0	3	0	0	54	0	0	0	7,052	0	92	0	35	0	0	0	7,748
W-V	0	0	12	0	0	0	0	0	0	0	0	0	0	0	460	0	0	0	0	0	472
W-P	0	0	133	0	500	0	0	1	0	0	0	0	0	0	803	2,393	0	0	22	38	3,890
P-P	2	182	26	0	337	0	0	0	0	13	0	142	0	398	0	176	0	1,062	415	870	3,623
NC	369,667	0	829	1,102	0	0	0	0	767	0	0	0	960	0	0	0	0	0	0	0	373,325
Total	370,967	2,234	2,780	2,267	5,107	15	13	1	3,331	97	1,082	190	8,017	398	1,374	2,569	36	1,062	462	922	

(UB: built-up areas; V: vegetation; P: paddy; W: water; BL: barren land)

Table 3. Confusion matrix of change type determination in land cover change detection improved with the third image

Classified data	Reference data																				
	NC	BL-UB	BL-V	BL-W	BL-P	UB-BL	UB-V	UB-P	V-BL	V-UB	V-W	V-P	W-BL	W-UB	W-V	W-P	P-BL	P-UB	P-V	P-P	Total
BL-UB	51	1,312	100	0	0	0	0	0	0	80	0	0	0	0	0	0	0	0	0	0	1,543
BL-V	31	~~389~~	1,057	0	0	0	4	0	0	0	0	0	0	0	3	0	0	0	0	0	1,484
BL-W	401	0	0	804	0	0	0	0	111	0	9	0	5	0	0	0	1	0	0	0	1,331
BL-P	61	~~450~~	468	0	4,270	0	9	0	0	4	0	48	0	0	16	0	0	0	25	14	5,365
V-BL	298	0	0	0	0	12	0	0	2,399	0	0	0	0	0	0	0	0	0	0	0	2,709
V-W	0	0	0	361	0	0	0	0	0	0	1,073	0	0	0	0	0	0	0	0	0	1,434
W-BL	456	0	56	0	0	3	0	0	54	0	0	0	7,052	0	92	0	35	0	0	0	7,748
W-V	0	0	12	0	0	0	0	0	0	0	0	0	0	0	460	0	0	0	0	0	472
W-P	0	0	133	0	500	0	0	1	0	0	0	0	0	0	803	2,393	0	0	22	38	3,890
P-P	2	~~182~~	26	0	337	0	0	0	0	13	0	142	0	398	0	176	0	1,062	415	870	3,623
NC	369,667	0	829	1,102	0	0	0	0	767	0	0	0	960	0	0	0	0	0	0	0	373,325
Total	370,967	2,234	2,780	2,267	5,107	15	13	1	3,331	97	1,082	190	8,017	398	1,374	2,569	36	1,062	462	922	

(UB: built-up areas; V: vegetation; P: paddy; W: water; BL: barren land)

Table 4. Accuracy for detecting changes from barren land to built-up areas

	Detection using the first and second images	Detection improved using the third image
Detection accuracy (%)	78.61	85.03
False-alarm rate (%)	0.25	0

Overall error rate (%)	0.34	0.06

5. Conclusions

This study developed a new method for monthly monitoring of land cover changes from barren land to built-up areas using RADARSAT-2 PolSAR images. The new method could significantly reduce the effect of seasonal vegetation growth on the detection of changes from barren land to built-up areas. Three sequential repeat-pass RADARSAT-2 PolSAR images were used in the new method. Change detection between the first and second images was made to detect monthly land cover changes, and then the change detection result was improved by reducing the confusion between changes to built-up areas and changes caused by seasonal vegetation growth using the interferometric coherence extracted from the second and third images. In change detection of the first and second images, seasonal paddy or vegetation growth produced many false alarms to changes from barren land to built-up areas because paddies and some natural vegetation were easily confused with buildings due to the similar scattering mechanism. The interferometric coherence extracted from the second and third images was used to improve the change detection result of the first and second images by reducing the false alarms caused by seasonal paddy and vegetation growth. Within the repeat cycle of RADARSAT-2, paddies and vegetation significantly lost coherency as a result of growth and changing moisture conditions, while the coherency of built-up areas remained high. Using the interferometric coherence, the detection accuracy for changes from barren land to built-up areas increased from 78.61% to 85.03%, while the false alarm rate reduced from 0.25% to 0%. The results showed that interferometric coherence significantly reduced the effect of seasonal vegetation growth and RADARSAT-2 PolSAR images were effective in monitoring monthly land cover changes from barren land to built-up areas.

References

Bovolo, F., and Bruzzone, L. (2007). A theoretical framework for unsupervised change detection based on change vector analysis in the polar domain. IEEE Transactions on Geoscience and Remote Sensing, 45, 218-236.

Gao, Y., Mas, J.F., Maathuis, B.H.P., Zhang, X.M., and Van Dijk, P.M. (2006). Comparison of pixel-based and object-oriented image classification approaches - a case study in a coal fire area, Wuda, Inner Mongolia, China. International Journal of Remote Sensing, 27, 4039-4055.

Lee, J.S., Wen, J.H., Ainsworth, T.L., Chen, K.S., and Chen, A.J. (2009). Improved sigma filter for speckle filtering of SAR imagery. IEEE Transactions on Geoscience and Remote Sensing, 47, 202-213.

López-Martínez, C., Ferro-Famil, L. and Pottier, E. (2005). PolSARpro v4.0 Polarimetry Tutorial, URL: http://earth.esa.int/polsarpro/tutorial.html, European Space Agency, Paris, France.

Lu, D., Mausel, P., Brondizio, E., and Moran, E. (2004). Change detection techniques. International Journal of Remote Sensing, 25, 2365-2407.

Malila, W. A. (1980). Change vector analysis: an approach for detecting forest changes with Landsat. Proceeding of Remotely Sensed Data symposium (pp. 326–336), W. Lafayette.

Moon, T.K. (1996). The expectation-maximization algorithm. IEEE Signal Processing Magazine, 13(6), 47-60.

Papathanassiou, K. P. and Cloude, S. R. (2001) Single-baseline polarimetric SAR interferometry, IEEE Transactions on Geoscience and Remote Sensing, Vol. 39, No. 11, 2352-2363.

Pierce, L. E., Ulaby, F. T., Sarabandi, K. and Dobson, M. C. (1994) Knowledge-Based Classification of Polarimetric Sar Images, IEEE Transactions on Geoscience and Remote Sensing, Vol. 32, No. 5, 1081-1086.

Qi, Z., Yeh, A.G.-O., Li, X., and Lin, Z. (2012). A novel algorithm for land use and land cover classification using RADARSAT-2 polarimetric SAR data. Remote Sensing of Environment, 118, 21-39.

Qi, Z. and Yeh, A.G.O. (2012). Integrating change vector analysis, post-classification comparison, and object-oriented image analysis for land use and land cover change detection using RADARSAT-2 polarimetric SAR images. In S. Timpf, and P. Laube (Eds.), Advances in Spatial Data Handling (107-123). Berlin: Springer.

Saatchi, S.S., Soares, J.V., and Alves, D.S. (1997). Mapping deforestation and land use in Amazon rainforest by using SIR-C imagery. Remote Sensing of Environment, 59, 191-202.

Ulaby, F. T., Kouyate, F., Brisco, B. and Williams, T. H. L. (1986) Textural Information in Sar Images, IEEE Transactions on Geoscience and Remote Sensing, Vol. 24, No. 2, 235-245.

Yeh, A.G.O. and Li, X. (1996). Urban growth management in the Pearl River Delta - an integrated remote sensing and GIS approach. ITC Journal, Vol. 1, 77-86.